HYBRID COMPUTER SIMULATION OF SPACE-TIME EFFECTS IN CANDU REACTORS USING A MODAL APPROACH

By

B. M. Monaghan[+], F. N. McDonnell[++], H. W. Hinds[+++]

PRESENTED AT THE SIMULATION SYMPOSIUM

ON REACTOR DYNAMICS AND PLANT CONTROL

ORANGEVILLE, ONTARIO, 1979 APRIL 18

[+] Canatom (Ontario) Ltd. Toronto, Ontario

[++] Atomic Energy of Canada Research Company, Ottawa, Ontario

[+++] Reactor Control Branch, Chalk River Nuclear Laboratories, Chalk River, Ontario

Hybrid Computer Simulation of Space-Time Effects in CANDU Reactors Using A Modal Approach

By

B. M. Monaghan, F. N. McDonnell and H. W. Hinds

Abstract

A hybrid computer model for the simulation of space-time reactor kinetics has been developed using the modal approach.

The modal approach consists of expressing all the relevant neutronic variables as a weighted sum of a base set of fixed natural-mode shape functions and a time-varying set of amplitude functions. The hybrid model was implemented to permit improved man-machine interaction and provide a real-time simulation capability. The various reactor transients studied included the effects of delayed neutron precursors, xenon-iodine dynamics, and a shut-down system. Comparison with an all digital code is good, within 1% to 2%.

The spatial behaviour of large CANDU reactor cores may now be included in the hybrid computer studies to assist engineers with control and safety analysis.

HYBRID COMPUTER SIMULATION OF SPACE-TIME EFFECTS IN CANDU REACTORS USING A MODAL APPROACH

By

B. M. Monaghan, F. N. McDonnell, H. W. Hinds

1. Introduction

An important part of the analysis of reactor safety and control system design is the accurate prediction of the spatial distribution of the neutron flux, during both steady state and transient conditions. As nuclear reactors increase in size, to benefit from economics of scale, the various regions throughout the core become less tightly coupled (1), and as a result, spatial dynamics effects become more important. Furthermore, present and future demands on CANDU-PHW reactor operation, such as on-line refuelling, improved load following capability and flattening of the power distribution lead to increased use of in-core reactivity devices. Sophistocated reactor models are required for the analysis of spatial flux reactivity transients resulting from manoevres of this sort.

Much work has been done in the area of reactor kinetics simulation, and an excellent summary of the techniques though somewhat dated, is given by Carter (2). Codes currently in use in CANDU reactor analysis include CERBERUS(3), based on the quasi-static approximation, SORGHUM(4), based on the adiabatic approximation and CHEBY(5), used for steady-state simulations. These codes all rely on computational procedures that are costly to run for realistic 3-D problems. Recently, an approach using the natural shapes of the neutron flux has been developed by Luxat(6) and implemented in the SMOKIN code. This model provides a good 3-D representation of the flux throughout the reactor at a greatly reduced cost.

To permit improved man-machine interaction and provide a real-time simulation capability, a hybrid computer model embodying the modal kinetic equations has been developed and implemented in parallel on the Dynamic Analysis Facility at CRNL(7). Results for a loss-of-coolant accident (LOCA) and xenon- dynamics simulations are presented in this paper. The good agreement obtained with an all-digital simulation and the intrinsic advantages that analog computation provides in system analysis lead to the conclusion that the hybrid computer model developed here will play an increasingly important role in control system and safety analysis.

2. The Hybrid Computer and Reactor Simulation

A hybrid system is essentially a combination of analog and digital computers, interfaced to provide high-speed transfer of information between them. In this way, the resulting hybrid system has the advantage of the analog computer of simultanious continuous integration of many ordinary or partial differential equations, and the advantage of the digital computer of sequentially performing many algebraic and logic operations at high speed. The high-level of interaction possible in analog computation allows the systems engineer to watch the solution unfold. He is able to get a "feel" for the dynamic nature of his problem.

The hybrid computer provides for rapid repetition of solutions, allowing the analyst to efficiently carry out parameter survey studies. Real-time simulation is attractive in that it permits the on-line testing of process-control equipment. In addition, the high-speed, low cost nature of analog integration results in economic incentives for the use of a hybrid system over its all-digital counterpart in the solution of differential equations.

Several methods have been developed for solving PDE by hybrid computers, and have been summarized by Vichnevetsky (8). These include coupled reactor models,such as that of Avery (9), and finite difference solutions. The use of finite differences to replace partial derivatives with respect to spatial variables gives rise to parallel methods, such as that of Hinds (10). A property of this method is that the required equipment complement increases in proportion to the desired accuracy, and has lead to the development of other techniques. An example is the continuous-space discrete-time (CDST) or Serial Method, where finite differences are used to replace the temporal derivatives. Because the analog circuit required for each finite difference node is basically the same, a single analog module may be used repeatedly throughout the core to increase the accuracy obtainable with the available component resources. With this technique, called multiplexing (10,11), the equations solved are discrete in both space and time. Storage and playback of intermediate values is required to generate the full space-time solution.

The hybrid computer has played an important role in the area of dynamic simulation at the Chalk River Nuclear Laboratories (12). The Dynamic Analysis Facility at CRNL is composed of a DEC PDP-11/55 digital-computer interfaced to two Applied Dynamics AD/FIVE analog computer consoles. Each console is capable of solving up to 30 simultaneous differential equations. In addition, a PDP-11/55 and PDP-8 are available for program development and auxiliary computer work.

The general layout of the system appears in figure 1. The computer hardware is supplemented by a number of software packages that facilitate off-line set-up and check-out as well as on-line function generation, storage and playback. The system is thus well equiped to handle full reactor simulations using the modal kinetics approach, including such effects as xenon-induced oscillations and power-feedback.

3. The Modal Reactor Kinetics Model

The modal expansion, or synthesis, methods consist of expressing all the relevant neutronic variables as weighted sums of a base set of fixed, spatial functions. A number of different approaches to this technique appear in the literature, and an excellent summary is provided by Stacey (13).

The set of spatial functions used to synthesize the flux originates in one of two ways. In the first case, the fundamental mode and higher harmonics are the eigen functions derived from a neutron-balance operator, such as that for the static diffusion equation, for the initial reactor configuration. A different approach is to use the solutions to neutron-balance equations applied to a perturbed reactor, thereby generating expansion functions tailored to represent the flux distortions anticipated for a particular transcient of interest. It is that set obtained using the former, more general method that is used for the simulations presented here.

We start by expanding the neutron flux, delayed neutron precursors, and iodine and xenon concentrations in terms of a base set of spatial eigenmodes ψ_i and time varying coefficients:

$$\phi(r,t) = \sum_{i=1}^{M} \psi_i(r) n_i(t) \qquad \text{......1a}$$

$$C_j(r,t) = \frac{1}{v} \sum_{i=1}^{M} \psi_i(r) C_{ij}(t) \qquad \text{......1b}$$

$$I(r,t) = \frac{1}{v} \sum_{i=1}^{M} \psi_i(r) I_i(t) \qquad \text{......1c}$$

$$X(r,t) = \frac{1}{v} \sum_{i=1}^{M} \psi_i(r) X_i(t) \qquad \text{......1d}$$

The mode shape functions ψ_i are the eigenfunctions of the static diffusion equation. With each mode is associated an eigenvalue $1/K_i$. Each of the higher harmonics is said to be subcritical relative to the fundamental, with the degree of subcriticality defined as:

$$\rho_{sci} = \frac{K_i - K_1}{K_1 K_i} \qquad \ldots\ldots 2$$

Typically, the fundamental mode is critical ie $K_1 = 0$. Only those modes with lower values of $|\rho sci|$ are likely to be excited enough by a given perturbation to be of any interest. We thereby justify the assumption that good accuracy may be obtained using a finite number of these modes. In fact, Luxat has shown (7) that for some transients only a few modes per spatial variable are required for adequate 3-D spatial representation of the flux. The model employed in the hybrid simulation presented here uses seven such modes, whose characteristic shapes and modal subcriticalities are shown in figure 2.

To obtain the modal kinetic equations, the modal expansion forms are substituted into the well known kinetic equations which describe the space-time behaviour of the pertinent variables. This equation set is reduced by the technique of Galerkin Weighting. The near orthogonality property of the modal eigenfunctions makes them the ideal weight factors. The Galerkin procedure consists of premultiplying equations (1) by the mode shape functions ψ_j and integrating the product terms over the volume of the reactor, yeilding an ordinary differential equation for each of the time dependant amplitudes. Details of this derivation are given in (6) and (7).

Recently a digital computer code, SMOKIN, which is based on the above formulation, has been developed by Luxat (14). Benchmark studies using proven codes have established the SMOKIN solutions as accurate and obtainable at greatly reduced costs.

To implement these equations on the hybrid computer, each variable must be scaled to its maximum value to prevent exceeding the fixed range of the analog amplifiers. As the equations are somewhat cumbersome, the modal kinetic equations and their scaled counterparts are given in the Appendix.

4. Implementation

One AD/FIVE console has a sufficient number of components to patch 7 flux modes, each with two active delayed neutron groups or alternatively the xenon-iodine mode amplitudes. In addition, the effects of reactivity devices and for power feedback are also included.

To fully explore the suitability of the modal model to hybrid simulation, two problem types over different time scales were implemented. The first simulation presented here is that of a loss-of-coolant accident (LOCA), which takes place over the order of several seconds. Here the dynamic effects of the delayed neutrons are important and two groups per mode were patched.

The effects of the LOCA voiding are represented by reactivities, both self-coupling (mode i to mode i) and cross-coupling (mode i to the fundamental and vise versa). The same is true for the shutdown system, so that a total of 38 function generations are required to supply these time-varying coefficients over the duration of the transient. The analog circuit layout for one of the higher modes is shown in figure 3. The boldface arrows indicate coefficient updating by the digital computer. The evolution of the voiding and shutdown system reactivities are shown in figure 4.

To set up the simulation, modal and neutronic data are read in by an off-line scaling program. The set of data used appears in TABLE I. Tables of the coupling coefficients for the LOCA and shutdown transient are prepared for the 'on the fly' function up-dating by the on-line run-time program (15). A set-up and check-out utility is used to set the coefficient devices and check the analog patching.

A similar procedure is carried out for the xenon-iodine dynamics simulation. The degree of non-linearity of the equations requires some of the multiplications to be done digitally. The analog schematics for the higher modes appear in figures 5a and 5b. Because the time scale of this type of problem is that of several hours, the dynamic effects of the delayed neutrons are practically negligable. Their presence is nonetheless accounted for by replacing the mean neutron life, ℓ^*, by ℓ', where (7)

$$\ell' = \ell^* + \sum_i \frac{\beta i}{\lambda i} \qquad .....3$$

Also included in this simulation were the effects of power feed-back.

5. Results

The hybrid computer solutions to the transients described above are shown in figures 6 and 7. The results were compared to those obtained using an all digital code FORSIM (17), and agreement within 1% to 2% was obtained. Considering the machine tolerances and the complexity of the equations,we feel that these results greatly support the use of the hybrid computer in this application.

Being able to observe the evolution of the flux mode amplitudes for the LOCA case, figure 6a, allows one to identify the tilt components in the distorted flux. To get a full spatial map of the flux at any time, the modal amplitude signals may be sampled and multiplied off-line by the spatial distribution functions. In this way the location of the maximum flux, or hottest bundle, may be determined.

Similarly for the xenon simulation, the oscillatory nature of the system's dynamics is clearly visible from the temporal behaviour of the xenon mode amplitudes, figure 7.

Parametric survey studies using the hybrid model were carried out, and some results are shown in figures 6b. In the LOCA simulation, the value of the final void worth was incremented by 5% of the nominal 4 mk. on consecutive runs to a maximum of 4.4 mk. The effect of varying the delay time to rod insertion, the trip set point and void location may likewise be observed. Again the results compare well with the digital benchmark.

The hybrid computer model is particularly well suited to frequency response measurements. A technique for measuring a systems transfer function using a pseudo random binary sequence and Fourier transformation has been developed at CRNL (18). A filtered PRBS signal is used to perturb the system in some way, which may represent, for example, jerking a control rod in and out of the core around some nominal value. The input and output are then sampled at some frequency, creating two tables. The tables are Fourier transformed, generating complex components in the frequency domain. Bode plots of the transfer functions obtained by complex division of the output by the input are of great use to the control system designer. They are also useful in evaluating the effects of simplifying assumptions.

Frequency response measurements on the two simulations are shown in figures 8a and 8b. A sample of the analog signals resulting from the PRBS excitation is shown in figure 8c. Note that a low frequency control loop is required to keep the system stable.

Consider the transfer function for mode i in the Laplace domain, where the fundamental mode is held near equilibrium (7).

$$G_i(s) = \frac{1}{s\ell^* + \sum_j \frac{s\,\beta j}{s + \lambda j} - \rho sci} \qquad \ldots\ldots 4$$

At low frequency this transfer function approaches a constant $\frac{1}{|\rho sci|}$. This result is clearly visible in figure 8a.

The above equation also implies that the effects of delayed neutrons should diminish with increasing values of $|\rho sci|$. This was also verified by experiment. Therefore the dynamics of the lower harmonics are more important, and this should be reflected in the distribution of the available analog components, ie more delayed neutron groups should be incorporated into the lower harmonics than into the higher ones.

6. Conclusion

A hybrid computer simulation, embodying the modal reactor kinetics equations, has been implemented and provides a useful means of studying reactor transients. The modal approach permits good 3-D representation of the main neutronic variables and is well suited to hybrid simulation. This simulation model, with improved man-machine interaction and real-time simulation capability, will play an important role in control system and safety analysis studies.

REFERENCES

(1) F.N. McDonnell and R.E. Green, "Spatial Control in Large Candu Reactors: The Whys and Wherefores", Paper presented at the 18th annual International Conference of the Canadian Nuclear Association, Ottawa, June, 1978. Also AECL 6212, Atomic Energy of Canada Limited, June, 1978.

(2) N.E. Carter "Review of Physics Methods Used for Computing the Kinetic Behaviour of Large Power Reactors", BNWL-738, Battelle Northwest (1958).

(3) G. Kugler and A.R. Dastur "Accuracy of the Improved Quasistatic Space-time Method Checked with Experiment", Trans. Am. Nucl. Soc., 23, 595 (1976).

(4) P. Akhlar and O.A. Trojan, "Xenon-Induced Power Oscillations in CANDU", Trans. Am. Nucl. Soc. 23, 596 (1976).

(5) A.M. Lopez, V.K. Mohindra, and J.R. Enselmoz, "Reactor Physics Measurements at Bruce GS A", Proc. 8th Biennial Topical Conference on Reactor Operating Experience, Chatanooga, Tennessee, August,1977.

(6) J.C. Luxat, "A Modal Kinetics Approach to Reactor Dynamics for Spatial Control Studies", Proceeding 1976 Simulation Symposium on Reactor Dynamics and Plant Control, AECL, Power Projects, TDAI-98, 1976.

(7) B.M. Monaghan, "Simulation hybride d'un modèle modal employé en dynamique des réacteurs nucléaires", Master's degree thesis, Ecole Polytechnique, Montreal.

(8) R. Vichnevetsky, "Analog/Hybrid Solution of Partial Differential Equations in the Nuclear Industry", Proceedings of the International Symposium on Analog and Hybrid Computation, Versailles, 1968.

(9) R. Avery, "Theory of Coupled Reactors", Procedures of the International Conference on Peaceful Uses of Atomic Energy, Geneva, 12, 182, 1958.

(10) H.W. Hinds, "A Hybrid Computer Simulation of Reactor Spatial Dynamics", Paper presented at the Third Power Plant Dynamics, Control and Testing Symposium, Knoxville, Tennessee, September, 1977.

(11) S.K.T. Hsu and R.M. Howe "Preliminary Investigation of a Hybrid Method for Solving Partial Differential Equations" Proceedings of the Fall Joint Computer Conference, 1968.

(12) R.E. Green, "Dynamic Analysis and Simulation at Chalk River", Part of "AECL Research and Development in Engineering", Special Edition 1976, Atomic Energy of Canada Limited, AECL-5550.

References (continued)

(13) W.M. Stacey Jr., "Space and Energy Dependant Neutronics in Reactor Transient Analysis" Reactor Technology, Vol 14, No. 2, 1977.

(14) J.C. Luxat, "The Potential of a Generalized Modal Analysis Method is the Design and Analysis of CANDU-PHW Reactor Control and Safety Systems", Paper presented at the 18th Annual International Conference of the Canadian Nuclear Association, Ottawa, 1978.

(15) B.M. Monaghan, "Modal Reactor Kinetics", Internal Unpublished Engineering File, Chalk River, Atomic Energy of Canada Limited, 1978.

(16) C. Lawrence and J. Barker "A Set-up and Check-out Utility", Proceedings of the Simulation Symposium on Reactor Dynamics and Plant Control, WNRE, Atomic Energy of Canada Limited, 1978.

(17) M.B. Carver et al. "The FORSIM VI Simulation Package for the Automated Solution of Arbitrarily Defined Partial and/or Ordinary Differential Equation Systems," Atomic Energy of Canada Limited, AECL 5821.

(18) C.B. Lawrence and A. Pearson, "Measurement Techniques Using a Pseudo-Random Binary Sequence and Fourier Transformation for Determining a System's Transfer Function," Atomic Energy of Canada Limited AECL-3601, April 1970.

TABLE I NEUTRONIC DATA

Description		Value
Delayed Neutron Data		
	β_1	0.004556
	β_2	0.003212
	λ_1	0.6871 s^{-1}
	λ_2	0.06297 s^{-1}
	ℓ^*	0.00092
Xenon-Iodine Data		
	γ_I	0.023703
	γ_X	0.0021156
	λ_I	0.0000294 s^{-1}
	λ_X	0.000021 s^{-1}
	ℓ'	0.536

Note: γ_I and γ_X are fractional yields for I^{135} and X^{135} normalized by ν

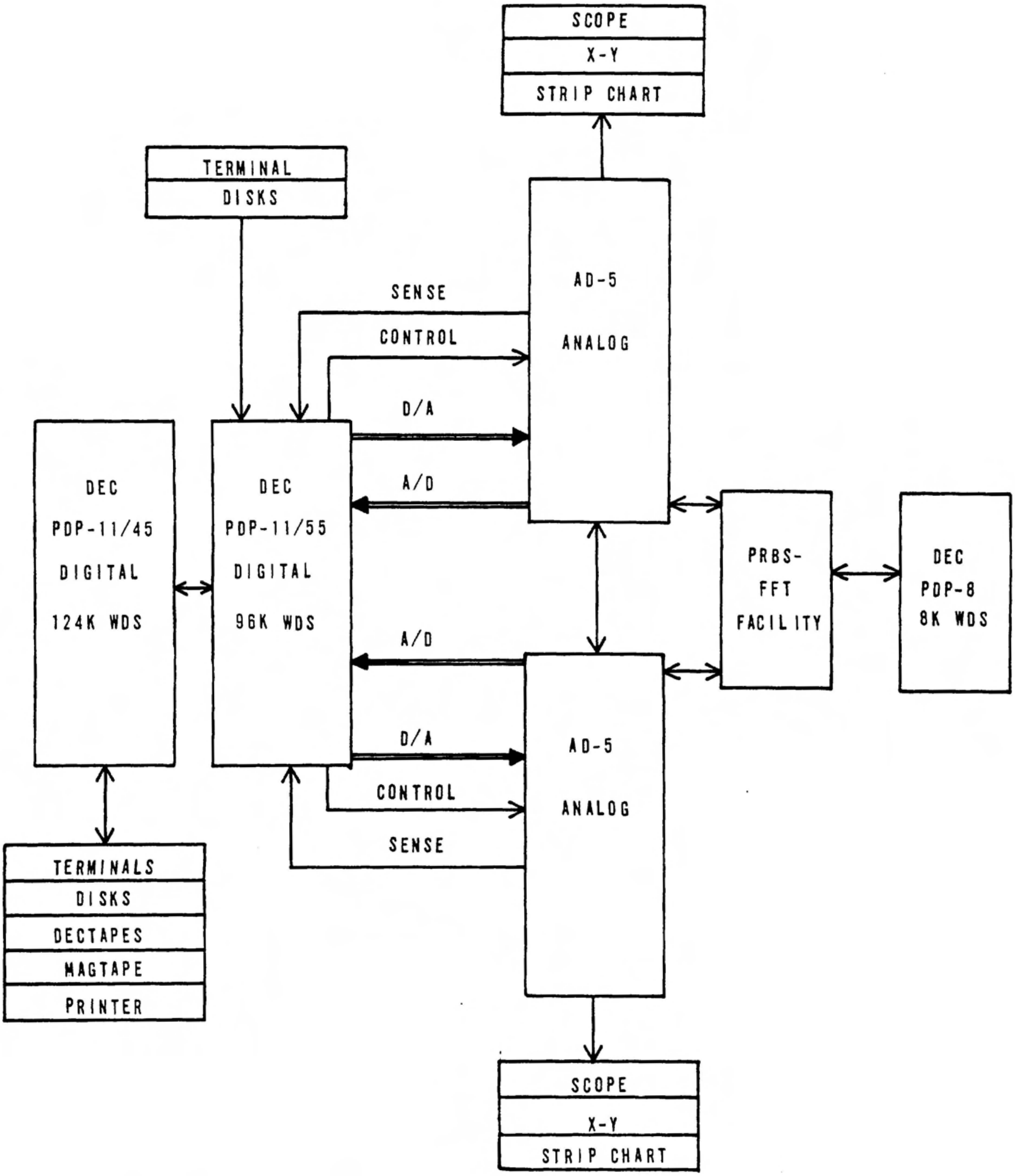

Figure 1: THE DYNAMIC ANALYSIS FACILITY AT CRNL

MODE NUMBER	MODE SHAPE (VIEWED FROM EAST FACE)		SUBCRITICALITY (mk)
1	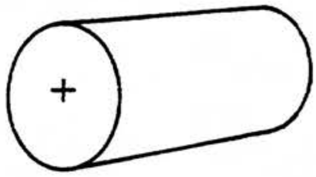	FUNDAMENTAL	0.0
2	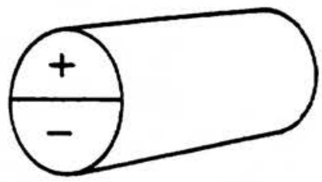	1st AZIMUTHAL TOP/BOTTOM	-13.326
3	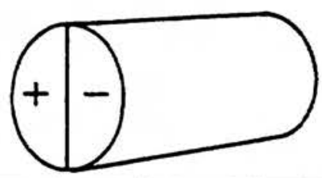	1st AZIMUTHAL SIDE/SIDE	-12.829
4	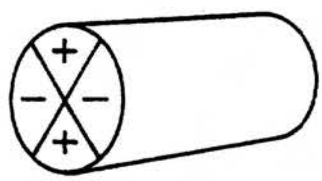	2nd AZIMUTHAL DIAGONAL	-33.509
5	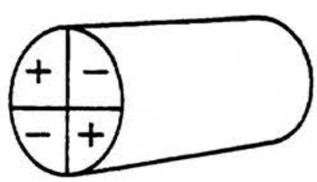	2nd AZIMUTHAL HORIZONTAL/ VERTICAL	-34.941
6	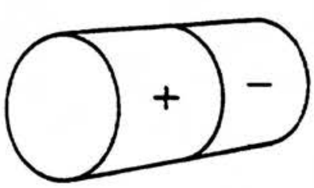	1st AXIAL	-21.223
7	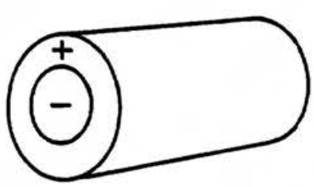	1st RADIAL	-48.690

Figure 2: SCHEMATIC REPRESENTATION OF FLUX MODE SHAPES

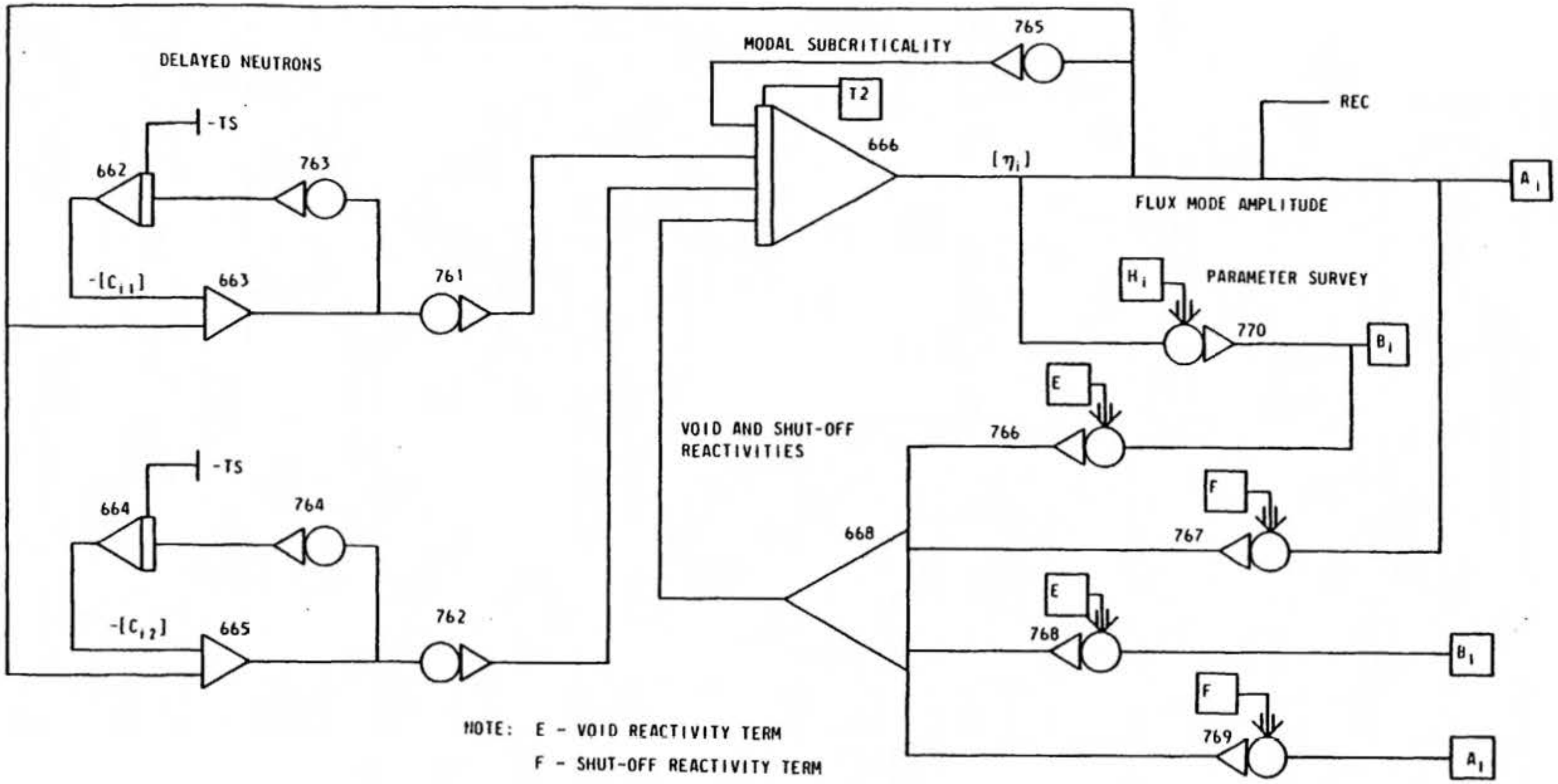

Figure 3: ANALOG CIRCUIT LAYOUT FOR ONE OF THE HIGHER MODES FOR THE LOCA SIMULATION

<u>Coefficient Index</u>

761	$\frac{\beta_1}{\ell^*}$	763	λ_1	765	$\frac{\rho_{sci}}{\ell^*}$
762	$\frac{\beta_2}{\ell^*}$	764	λ_2	766–769	Void and Shutoff Reactivities

VOID REACTIVITY

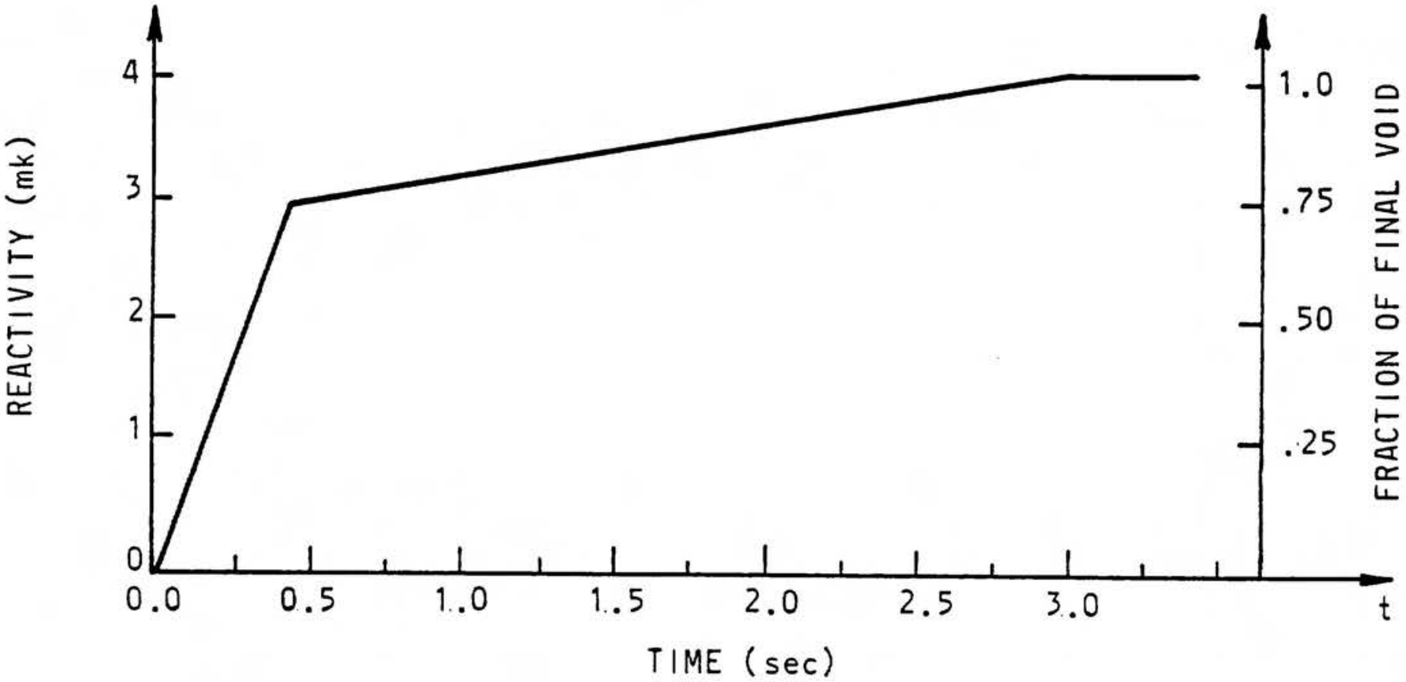

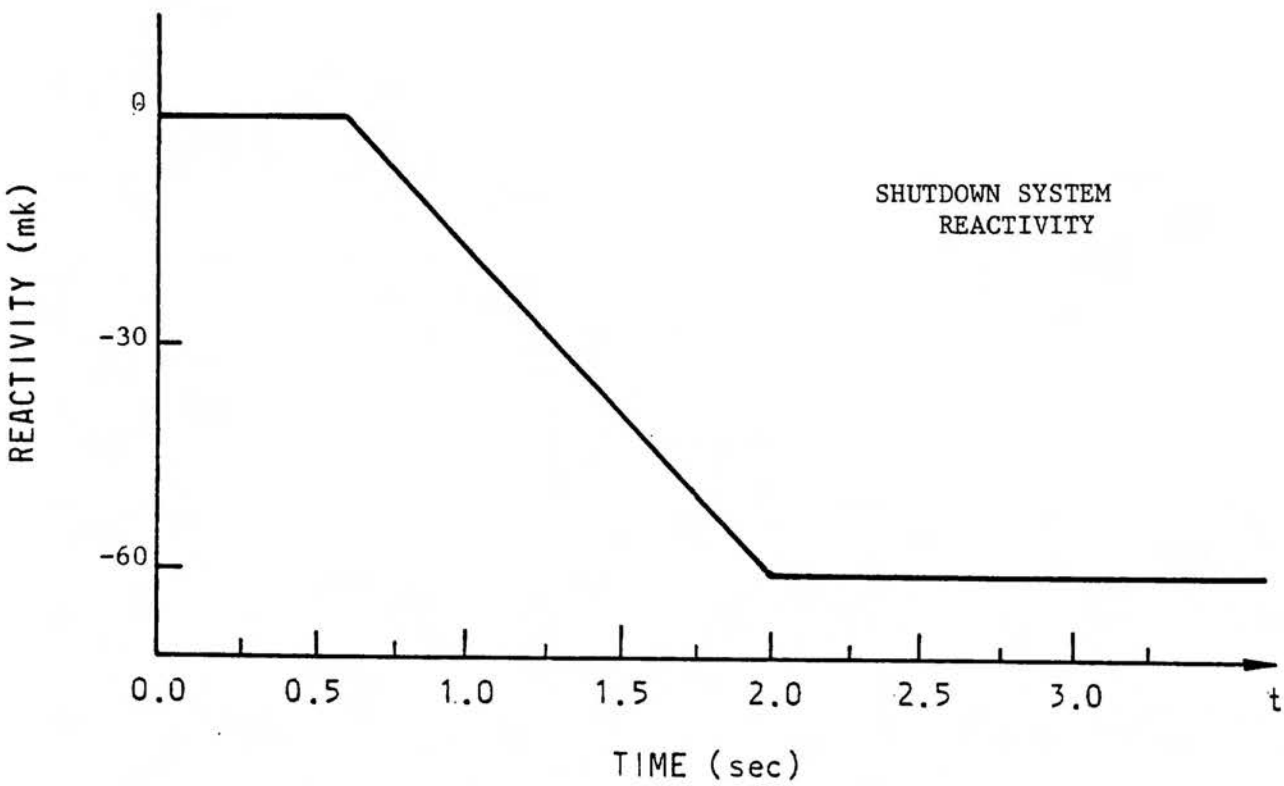

Figure 4: VOIDING AND SHUTDOWN SYSTEM REACTIVITY TRANSIENTS

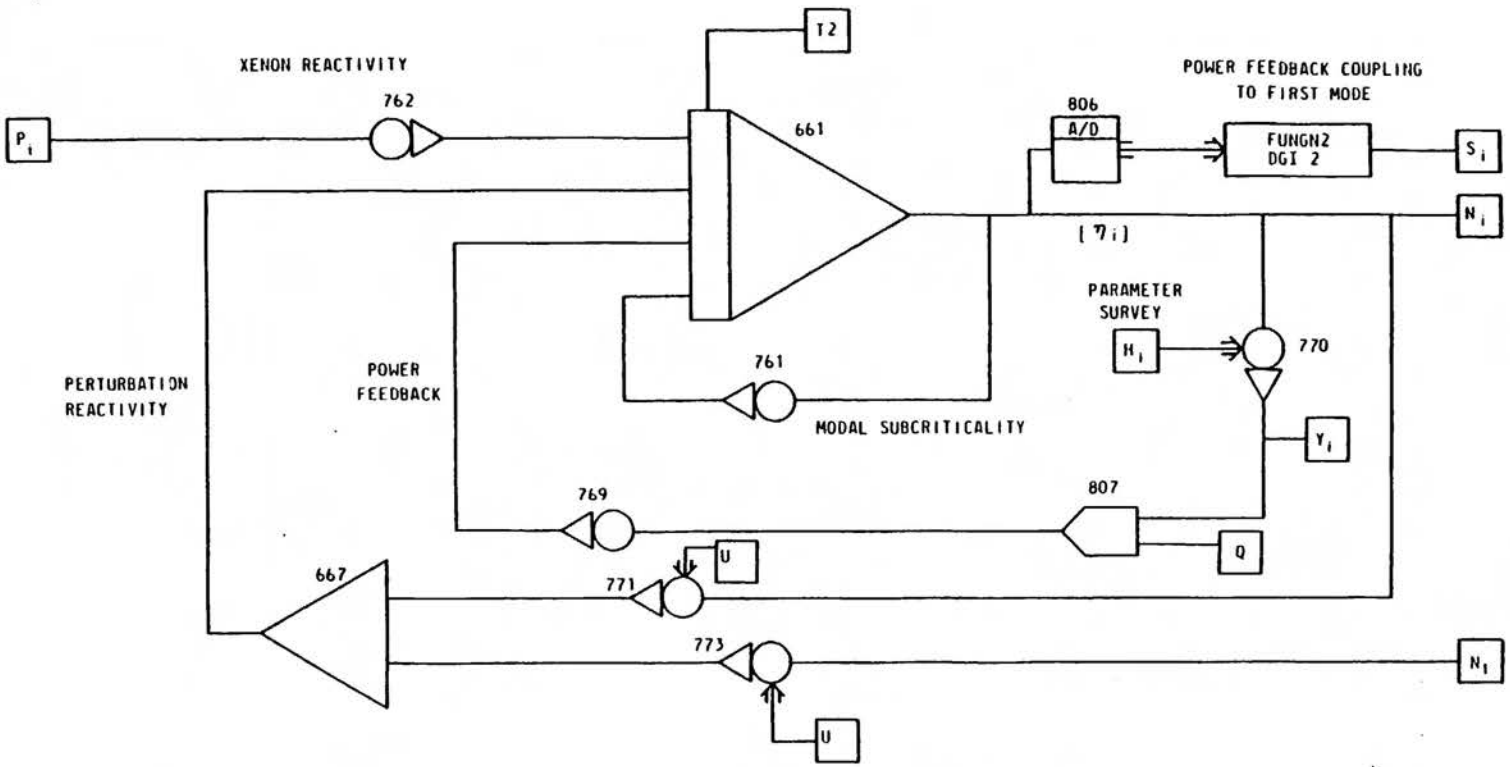

<u>Coefficient Index</u>

761 $\frac{B}{\ell'}$ ρ_{sci}

762 $BF_i R\delta\eta_1 max$

769 $\frac{B}{\ell'}$ ρ_{FBi}

Figure 5a:

Analog Circuit Layout for one of the Higher Modes
for the Xenon Simulation, Part I

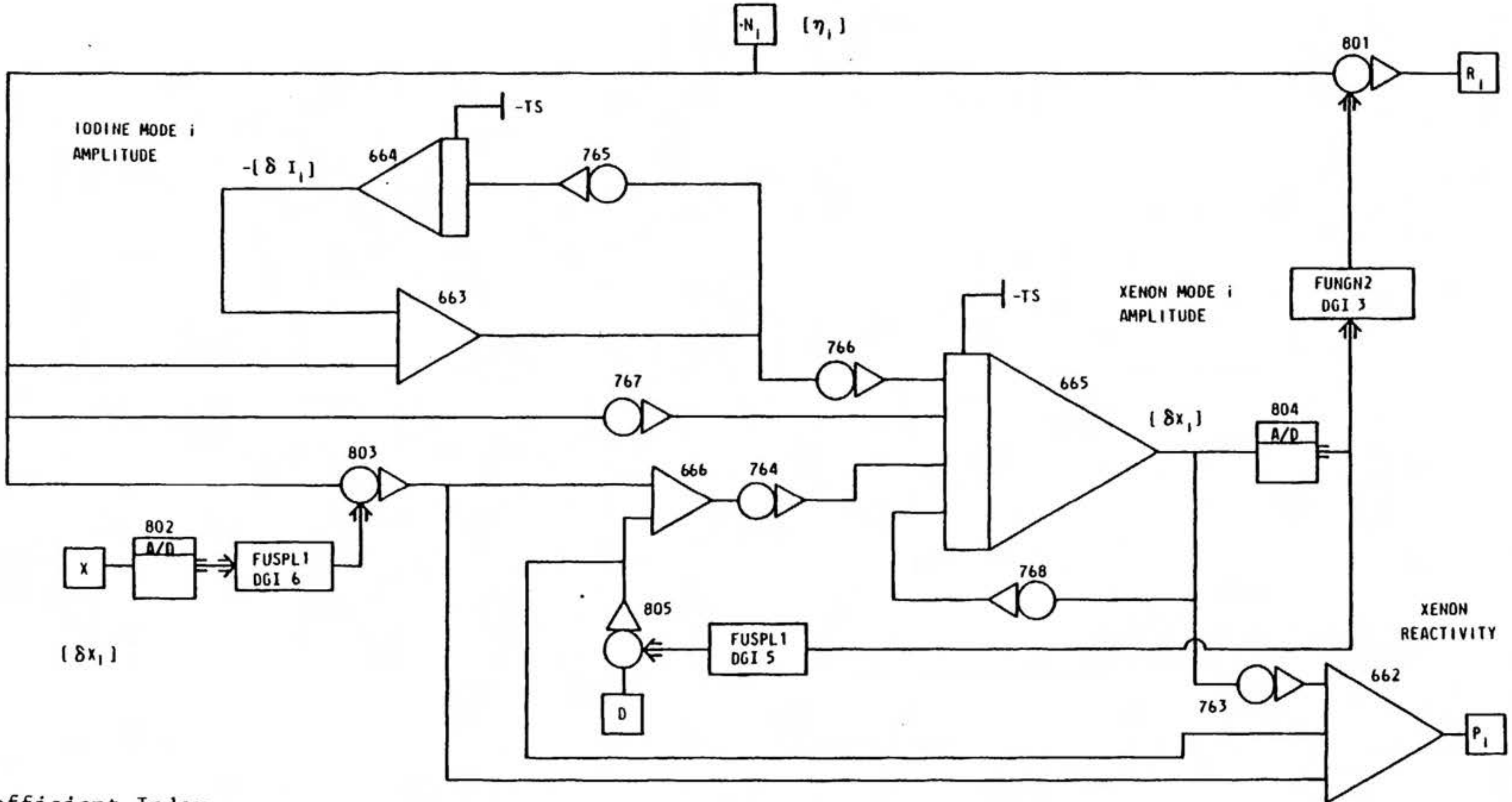

Coefficient Index

764	$BF_i\delta\eta_1 max$	768	$B(\lambda_X + F_i\eta_{01})$
765	$B\lambda_I$		
766	$\dfrac{B\gamma_I(\lambda_X + F_1\eta_{01})}{a(\gamma_X + \gamma_I)}$		
767	$\dfrac{B}{a}(\lambda_X + \eta_{01}(F_1 - F_i))$		

Figure 5b:

Analog Circuit Layout for one of the Higher Modes

for the Xenon Simulation, Part II

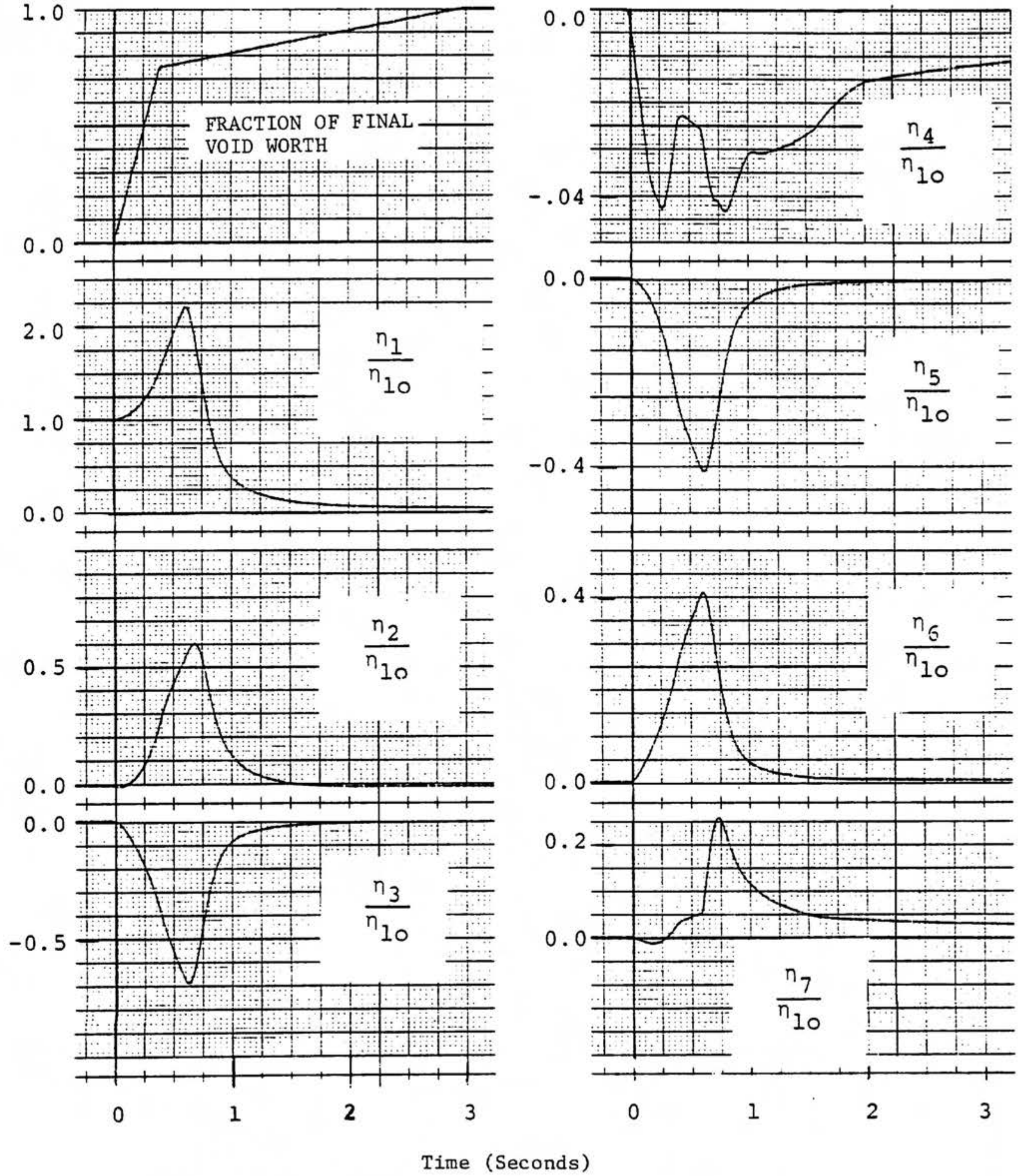

Figure 6a: Analog outputs for the Loca transient

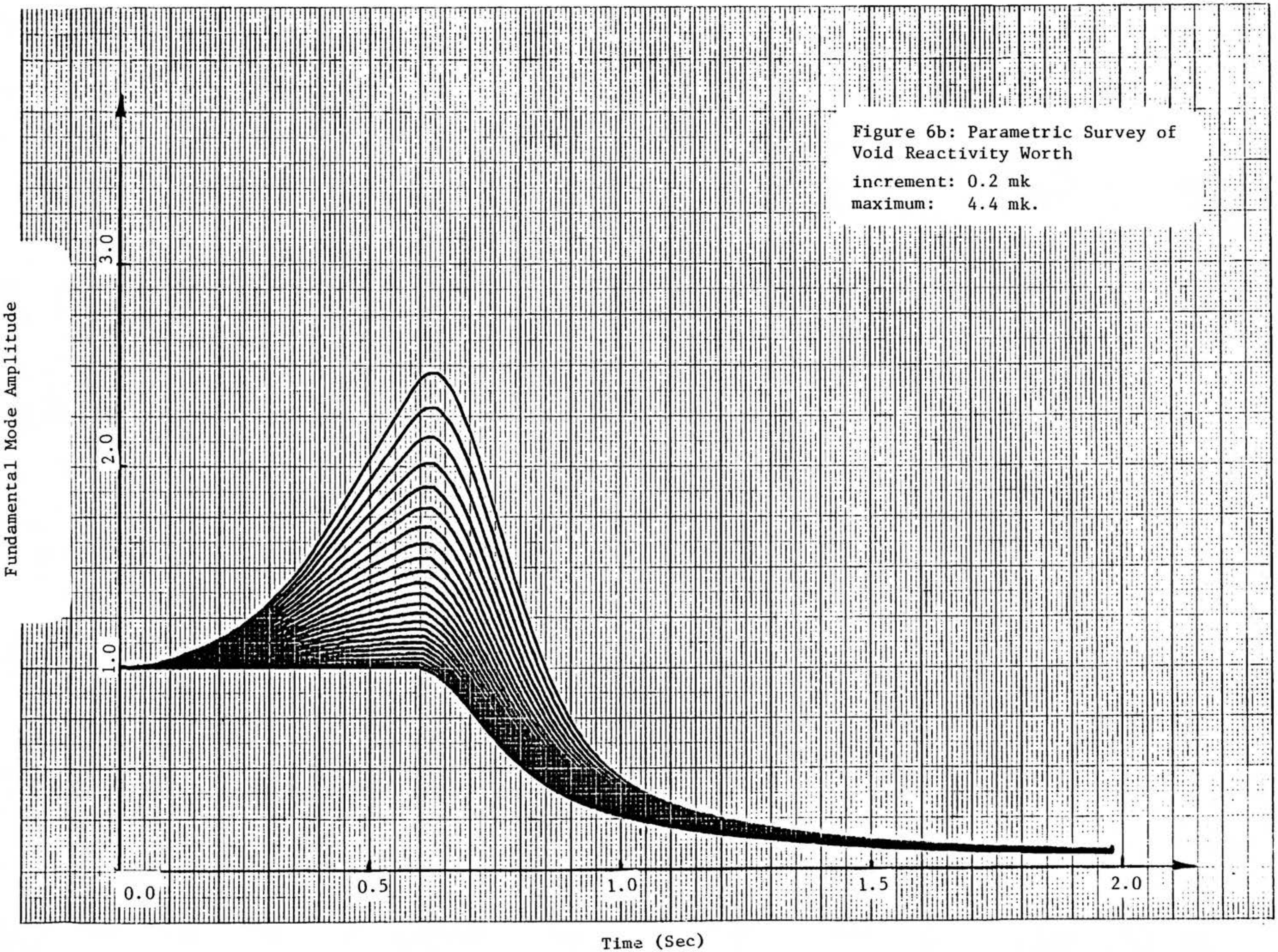

Figure 6b: Parametric Survey of Void Reactivity Worth

increment: 0.2 mk
maximum: 4.4 mk.

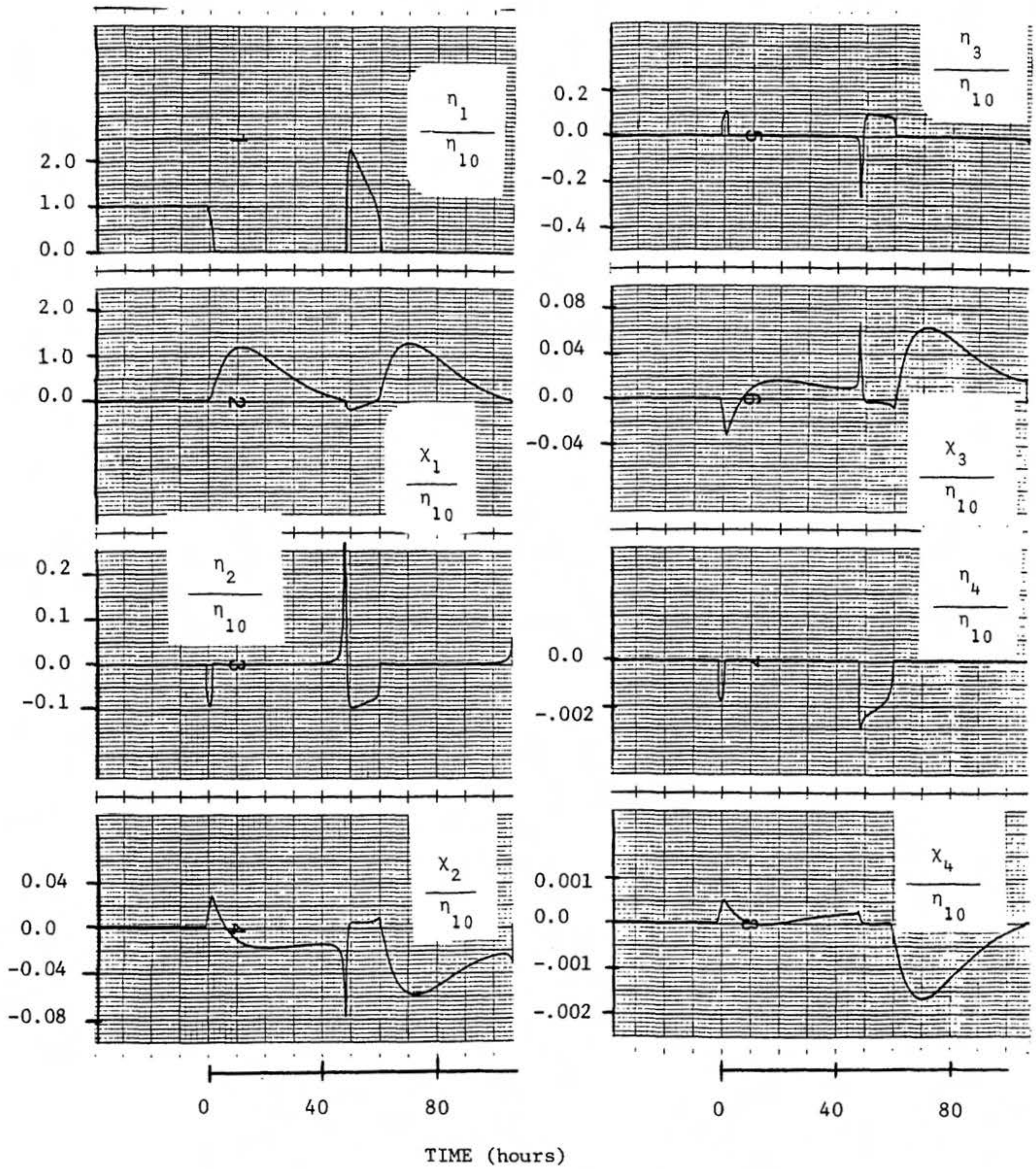

Figure 7: Flux and Xenon Mode Amplitudes for the Xenon Simulation

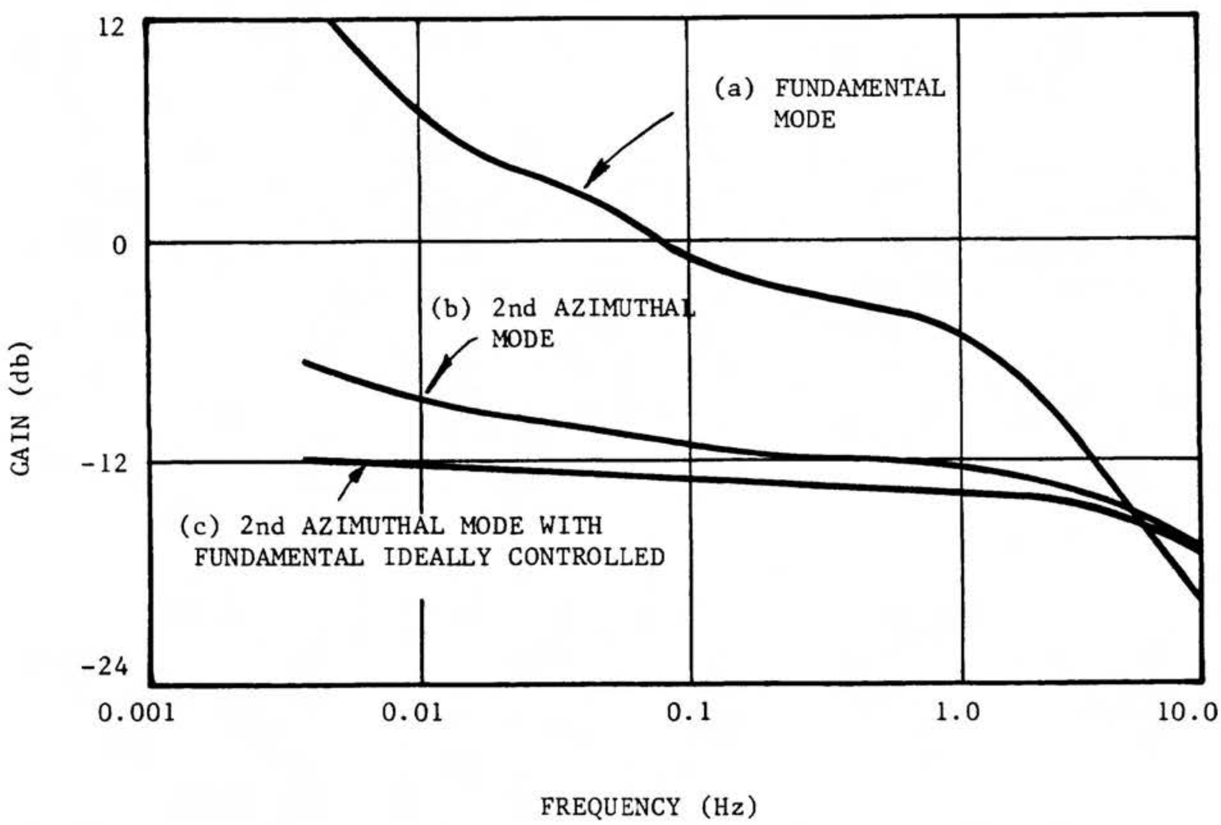

Figure 8a: Normalized Frequency Response of Mode Flux Amplitude To The Water Level In 1 Of 14 Zonal Control Elements in CANDU-PHW Reactor

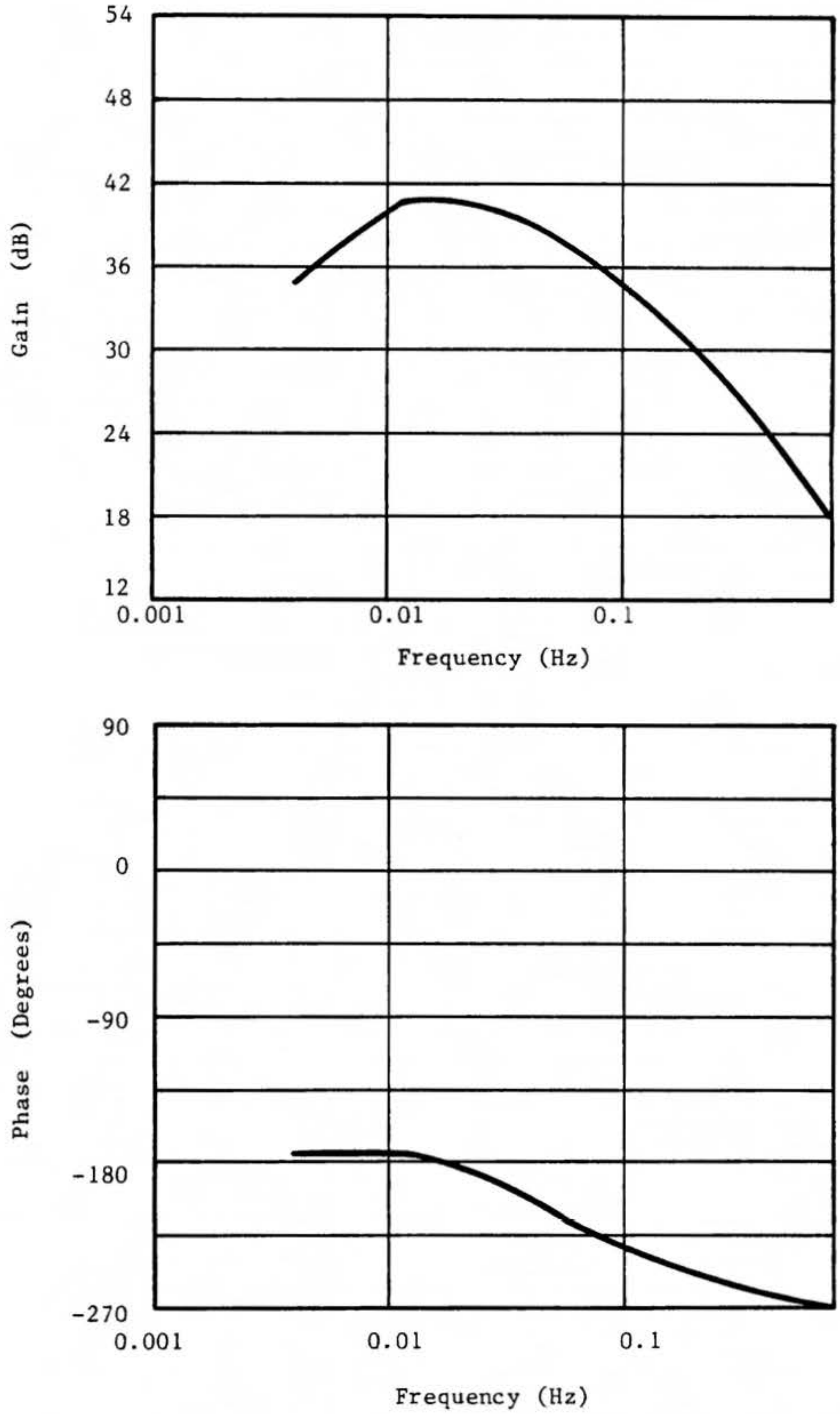

Figure: 8b Normalized Frequency Response of 1st Azimuthal Xenon Mode Amplitude to water level in 1 of 14 Zonal Control Elements in CANDU-PHW Reactor.

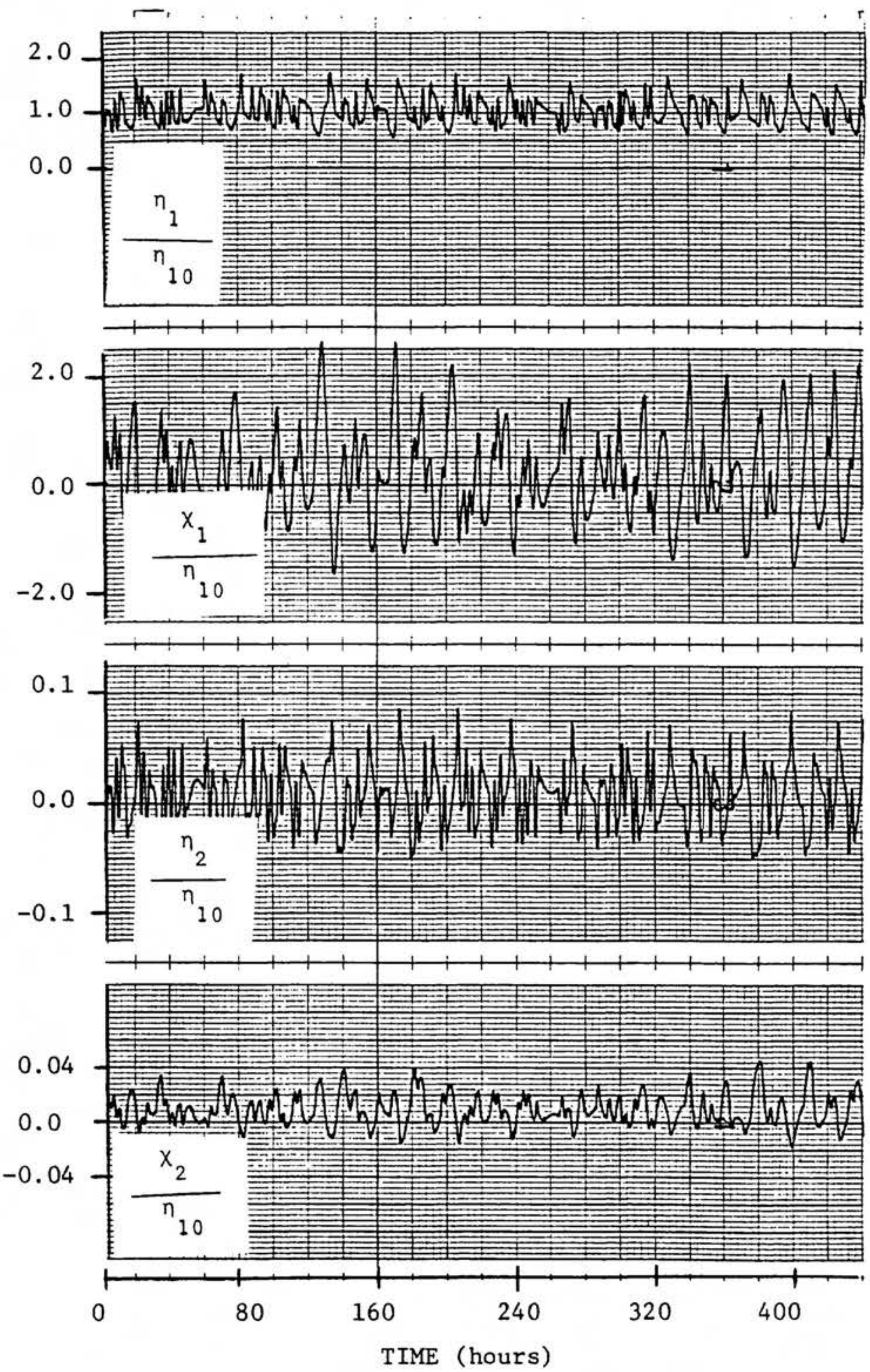

Figure 8c: Flux and Xenon Mode Amplitude Response to PRBS excitation of one of 14 Zonal Control Elements in a CANDU-PHW Reactor

APPENDIX

The modal kinetic equations and their scaled counterparts are presented here. For more details, consult the references (7), (14), (15). The nomenclature at the end of this appendix gives a brief description of the variables used.

The kinetic equations for the modal amplitudes of the main dynamic variables are given below.

$$\frac{\partial n_i}{\partial t} = \frac{(\rho_{sci} + \rho_{ii} - \beta)}{\ell^*} n_i + \frac{\rho_{i1}}{\ell^*} n_1$$

$$+ \sum_{j=1}^{D} \lambda_j C_{ij} + \frac{\sigma_{xi}}{B_i} (\Delta X_i n_1 + \Delta X_1 n_i)$$

$$+ \frac{\rho_{FB_i}}{\ell^*} (\Delta n_1 n_i + \Delta n_i n_1) \qquad \text{..........A1a}$$

$$\frac{\partial C_{ij}}{\partial t} = -\lambda_j C_{ij} + \frac{\beta_j}{\ell^*} n_i \qquad \text{..........A1b}$$

$$\frac{\partial I_i}{\partial t} = -\lambda_I I_i + \frac{\gamma_I}{\ell^*} n_i \qquad \text{..........A1c}$$

$$\frac{\partial X_i}{\partial t} = -\lambda_x X_i + \lambda_I I_i + \frac{\gamma_x}{\ell^*} n_i \qquad \text{..........A1d}$$

$$-\frac{\sigma_{xi}}{Bi} (X_i n_1 + X_1 n_i)$$

As is always the case with analog computation, each variable must be scaled to avoid exceeding the fixed range of the amplifiers. We shall use curly brackets to denote variables scaled to their maxima, ie:

$$\{n_i\} = \frac{n_i}{n_i max} \qquad \text{..........A2}$$

A1. The Scaled Equations for the LOCA Simulation

Dividing the variables in equations A1. by their maxima and rearranging, we find:

$$\frac{d}{dt}\{\eta_i\} = \frac{\rho_{sci}}{\ell^*}\{\eta_i\} + \frac{\rho_{ii}}{\ell^*}\{\eta_i\} + \frac{\rho_{i1}}{\ell^* S_i}\{\eta_1\} + \sum_{j=1}^{ND}\frac{\beta_j}{\ell^*}\{P_{ij}\} \qquad \text{..........A3a}$$

$$\frac{d}{dt}\{C_{ij}\} = -\lambda_j\{P_{ij}\} \qquad \text{..........A3b}$$

$$\{P_{ij}\} = \{C_{ij}\} - \{\eta_i\} \qquad \text{..........A3c}$$

For the first mode, where couplings from all of the higher modes are present, the flux mode amplitude equation becomes:

$$\frac{d}{dt}\{\eta_1\} = \frac{\rho_{11}}{\ell^*}\{\eta_1\} + \frac{1}{\ell^*}\sum_{i=2}^{NM}\rho_{i1}\,S_i\,\{\eta_i\} + \sum_{j=1}^{ND}\frac{\beta_j}{\ell^*}\{P_{ij}\}$$

Here, the effects of xenon and power feedback have not been included. We have implicitly used the steady state relationship

$$P_{ij}\max = \lambda C_{ij}\max = \frac{\beta_j}{\ell^*}\,\eta_i\max \qquad \text{..........A4}$$

to reduce the equations. We have also introduced a scaling factor for each mode.

$$S_i = \frac{\eta_i\max}{\eta_1\max} \qquad \text{..........A5}$$

A2. The Scaled Equations for the Xenon Simulation

For the xenon and iodine concentrations, the so-called "backed-off" model is used; the concentrations are given by their deviations from an equilibrium reference condition. The reference condition is chosen here to be the intial condition.

$$\delta X_i(t) = X_i(t) - X_{io}$$

$$\delta I_i(t) = I_i(t) - I_{io}$$

$$\delta \eta_i(t) = \eta_i(t) - \eta_{io} \qquad \text{..........A6}$$

In this treatment of xenon dynamics, the delayed neutron terms are dropped. Their effect on the transfer function for the neutronics is nonetheless accounted for by replacing the mean prompt neutron lifetime, ℓ^*, by ℓ' as discussed in the text of the paper. We define for simplicity

$$F_i = \frac{\sigma x_i}{B_i} \qquad \text{..........A7}$$

and use the steady state relationships.

$$\frac{\delta \eta_{i\max}}{\delta I_i \max} = \frac{\lambda_I \ell'}{\gamma_I} \qquad \text{..........A8}$$

$$\frac{\delta \eta_{i\max}}{\delta X_{i\max}} = \frac{\ell'(\lambda_x + F_1 \eta_{01})}{a(\gamma_x + \gamma_I)} = \frac{1}{R}$$

Furthermore, we introduce

$$\tau = \frac{1}{B} t$$

where τ = computer (machine) time

and t = problem (real) time

B = time scaling factor

In view of these definitions, equations A1. reduce to:

$$\frac{d}{dt}\{\delta I_i\} = -B\lambda_I\left[\{\delta I_i\} - \{\delta\eta_i\}\right] \qquad \text{..........A9a}$$

$$\begin{aligned}\frac{d}{dt}\{\delta X_i\} = {} & -B(\lambda_x + F_i\eta_{01})\{\delta X_i\} \\ & -BF_i\delta\eta_{1max}\Big[\{\delta\eta_1\}\{\delta X_i\} \\ & \qquad + \{\delta\eta_i\}\{\delta X_1\}\Big] \\ & +\frac{B\gamma_I(\lambda_x + F_1\eta_{01})}{a(\gamma_x + \gamma_I)}\left[\{\delta I_i\} - \{\delta\eta_i\}\right] \\ & +\frac{B}{a}\left[\lambda_x + \eta_{01}(F_1 - F_i)\right]\{\delta\eta_i\} \qquad \text{..........A9b}\end{aligned}$$

$$\begin{aligned}\frac{d}{dt}\{\eta_i\} = {} & \frac{B}{\ell'}\left[\rho_{sci} + \rho_{ii} + \rho_{FBi(\{\eta_1\} + \{\delta\eta_1\})}\right]\{\eta_i\} \\ & +\frac{B}{\ell'}\frac{\rho_{i1}}{S_i}\{\eta_1\} \\ & +BF_iR\delta\eta_{1max}\Big[\{\delta X_1\}\{\eta_i\} + \\ & \qquad \{\delta X_i\}\{\eta_1\}\Big] \qquad \text{..........A9c}\end{aligned}$$

A3. Treatment of Reactivity Devices

As discussed in (6), local changes in absorption and fission cross-sections resulting from the presence of control devices or refuelling are represented by reactivity terms, where we write, for each perturbation concerned

$$\theta_{kij} = \frac{\langle\psi_K \,|\, (1-\beta)\Delta P_j - \Delta R_j \,|\, \psi_i\rangle \Delta v_j}{\langle\psi_K \,|\, P_0 \,|\, \psi_K\rangle} \qquad \text{..........A10}$$

where P_0 is the production operator at equilibrium and ΔP_j and ΔR_j are the perturbations due to device j. If several reactivity devices are present, we simply sum them to get the ρ reactivities

$$\rho_{ki} = \sum_j \theta_{kij} \qquad \text{..........A11}$$

Since we are only interested in the coupling terms to and from the first mode, we need to calculate θ_{iij}, θ_{i1j} and θ_{1ij} only.

A4. Nomenclature

Symbol	Item	Unit
Roman		
a	xenon mode amplitude scaling factor	dimensionless
B	time scaling factor	-
B_i	mode flux squared integral ratio, mode i	dimensionless
$C_{ij}(t)$	delayed neutron precursor group j mode amplitude for mode i	dimensionless
F_i	convenient constant used to replace $\frac{\sigma_{xi}}{B_i}$	cm^2
I_i	iodine 135 amplitude for mode i	dimensionless

NOMENCLATURE (continued)

Symbol	Item	Unit
Roman		
K_i	criticality of mode i	dimensionless
ℓ^*	mean neutron lifetime	s
ℓ'	corrected neutron lifetime at low frequency	s
P	production operator	-
r	spatial co-ordinate	-
R	removal operator	-
S_i	scaling factor for mode i, ie. $\eta_i = S_i\{\eta_i\}$	dimensionless
t	real time	s
v	mean neutron velocity	$cm \cdot s^{-1}$
Greek		
β	total delayed neutron fraction	dimensionless
β_j	fractional yield of delayed neutron group j	dimensionless
γ_I, γ_X	fractional yields for I^{135} and X^{135} normalized by ν	dimensionless
$\delta I, \delta X, \delta\eta$	deviations from equilibrium mode amplitudes for iodine, xenon and neutron flux	dimensionless
$\delta\eta_{1max}$	maximum deviation of neutron flux mode amplitude	dimensionless
η_i	neutron flux mode i amplitude	dimensionless
θ_{kij}	reactivity coupling mode i to mode k for device j	k
$\lambda_j, \lambda_I, \lambda_X$	decay constants for delayed group j, iodine 135 and xenon 135 respectively	s^{-1}

NOMENCLATURE (continued)

Symbol	Item	Unit
Greek		
ν	average number of neutrons released per fission	dimensionless
ρ_{sci}	mode i subciticality	k
ρ_{ii}	change in modal subciticality due to presence of perturbation	k
ρ_{FBi}	modal power feedback coefficient, mode i	$\frac{k}{100\%}$
σ_x	microscopic absorption cross-section for xenon 135	cm^2
σ_{xi}	xenon 135 modal absorption coefficient, mode i	cm^2
τ	scaled time	-
$\phi(r,t)$	neutron flux	$\frac{n}{cm^2 s}$
$\psi_i(r)$	mode i spatial distribution	$\frac{n}{cm^2 s}$
Subscripts		
o	initial condition	